Error and resolution properties of 2-D resistivity models from the inversion of DCR and RMT data

Thomas Kalscheuer[1]

[1]ETH Zürich, Institute of Geophysics, Switzerland

4/9/2009

Introduction

1. Application of novel model error and resolution analyses to single and joint inversion of DCR and RMT data.
2. Smoothness-constrained analysis:
   - Often, linearized measures of model error and resolution.
   - Validation with newly developed smoothness-constrained most-squares inversion.
3. Non-linear TSVD analysis:
   - How well is the model constrained by the data?
   - Non-linearity accounted for, smoothness constraints avoided.
   - Validation with TSVD based most-squares inversion

Linearized inverse theory I

Assumption

$$\mathbf{F}\left[\mathbf{m}^{true}\right] \approx \mathbf{F}\left[\mathbf{m}_k\right] + \mathbf{J}\left(\mathbf{m}^{true} - \mathbf{m}_k\right) \tag{1}$$

Model resolution matrix

$$\mathbf{m}_{k+1} \approx \mathbf{R}_M \mathbf{m}^{true} + \left(\mathbf{I} - \mathbf{R}_M\right)\mathbf{m}_r + \mathbf{J}_{\mathbf{W}}^{-g}\mathbf{n}_{\mathbf{W}} \tag{2}$$

with $\mathbf{R}_M = \mathbf{J}_{\mathbf{W}}^{-g}\mathbf{J}_{\mathbf{W}}$

Linearized inverse theory II

Model covariance matrix

$$[cov\ \mathbf{m}_{k+1}] \approx (\mathbf{I} - \mathbf{R}_M)\,[cov\ \mathbf{m}_r]\,(\mathbf{I} - \mathbf{R}_M)^T + \mathbf{J}_{\mathbf{W}}^{-g}\,\mathbf{J}_{\mathbf{W}}^{-g\,T} \tag{3}$$

- Parameter errors are square roots of diagonal entries of $[cov\ \mathbf{m}_{k+1}]$.
- Errors on $\log_{10}\rho$ are factors f on ρ, permitting range $\left[\frac{\rho}{f}, f\,\rho\right]$.
- Verification with smoothness-constrained most-squares inversion.

Non-linear TSVD resolution and variance estimates I

Scheme

- Solely data driven and without artefacts of smoothness constraints.
- Uses trade-off between model resolution and variance:
  - Keeps model errors under threshold f_{thresh}, i.e. computes a truncation level p_{cutoff} of TSVD.
  - Then, computes resolution properties for this truncation level.
- Approximates effect of non-linearity.

Non-linear TSVD resolution and variance estimates II

Iterative computation of variance and resolution for parameter k

- Variance

$$var\left(m^{est}_{k,p+1}\right) = var\left(m^{est}_{k,p}\right) + \frac{1}{\lambda^2_{p+1}} v^2_{k,p+1} \tag{4}$$

  Include more singular values $\Rightarrow$ increase variance.

- Resolution from k-th row of

$$\mathbf{R}_{p+1} = \mathbf{V}_{p+1}\mathbf{V}^T_{p+1} = \mathbf{V}_p\mathbf{V}^T_p + \mathbf{v}_{p+1}\mathbf{v}^T_{p+1} = \mathbf{R}_p + \mathbf{v}_{p+1}\mathbf{v}^T_{p+1} \tag{5}$$

  Include more eigenvectors $\Rightarrow$ improve resolution.

Non-linear TSVD resolution and variance estimates III

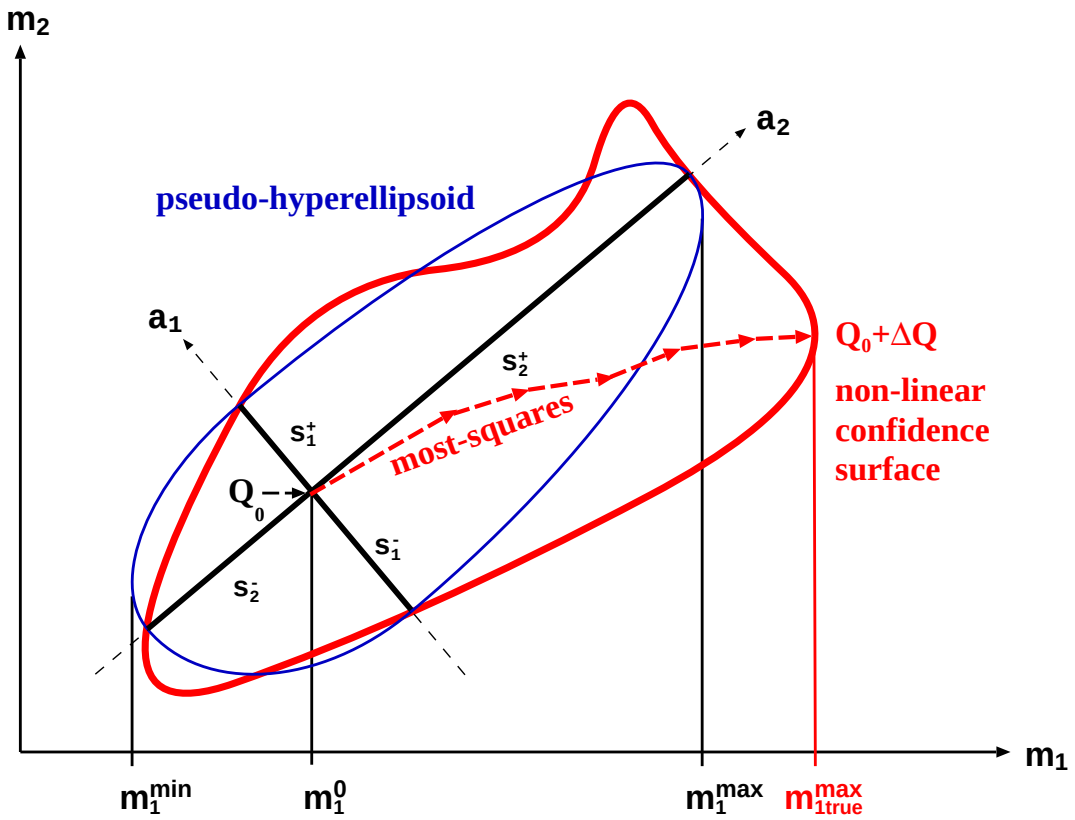

Figure: Pseudo-hyper-ellipsoidal surface as an approximation to the non-linear confidence surface (linear case $s_i = \sqrt{\Delta Q}/\lambda_i$) and most-squares iteration to true maximal model parameter.

2-D inverse modelling example

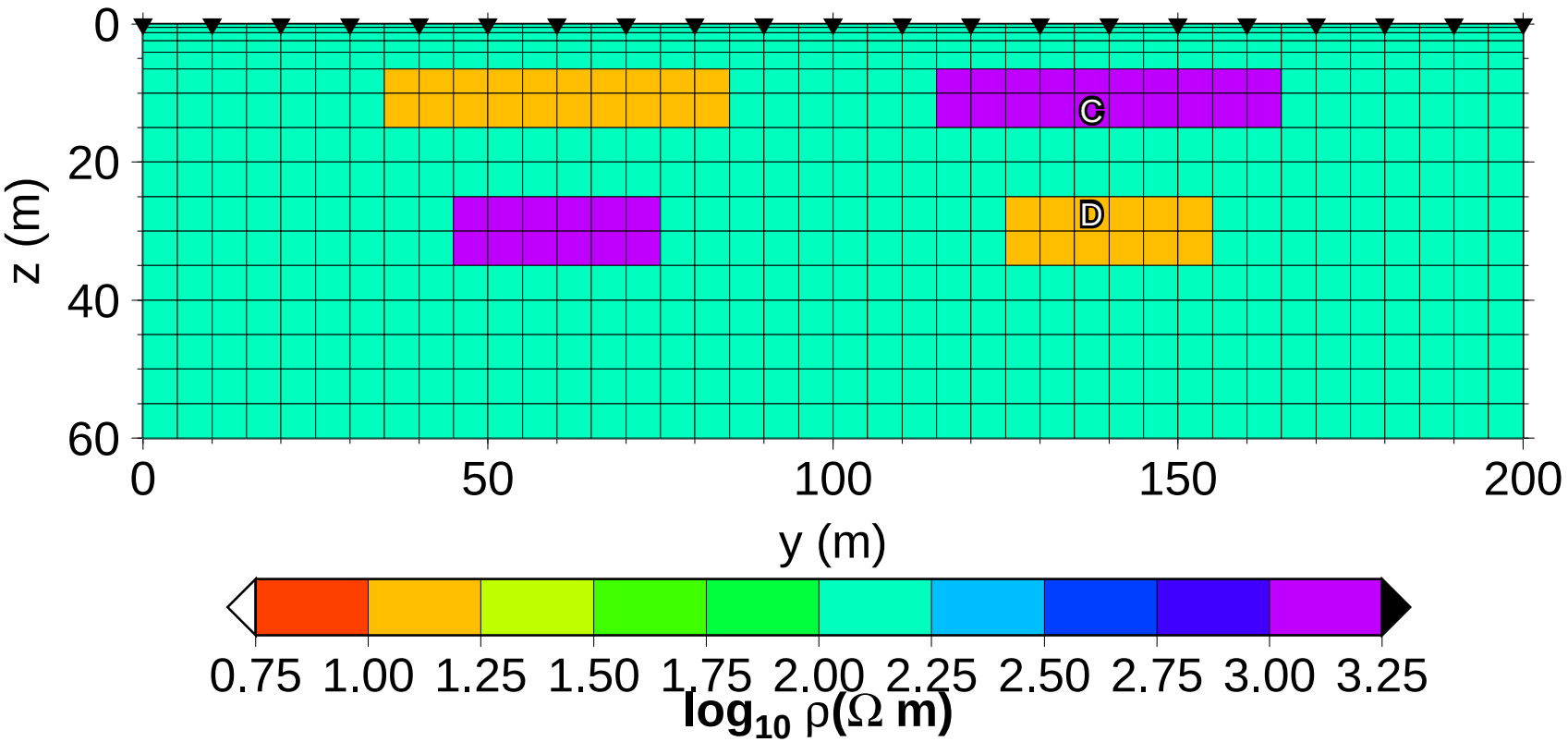

Figure: Model with buried blocks of 10 Ωm and 1000 Ωm in uniform host of 100 Ωm. DCR electrodes and RMT stations are indicated by black triangles.

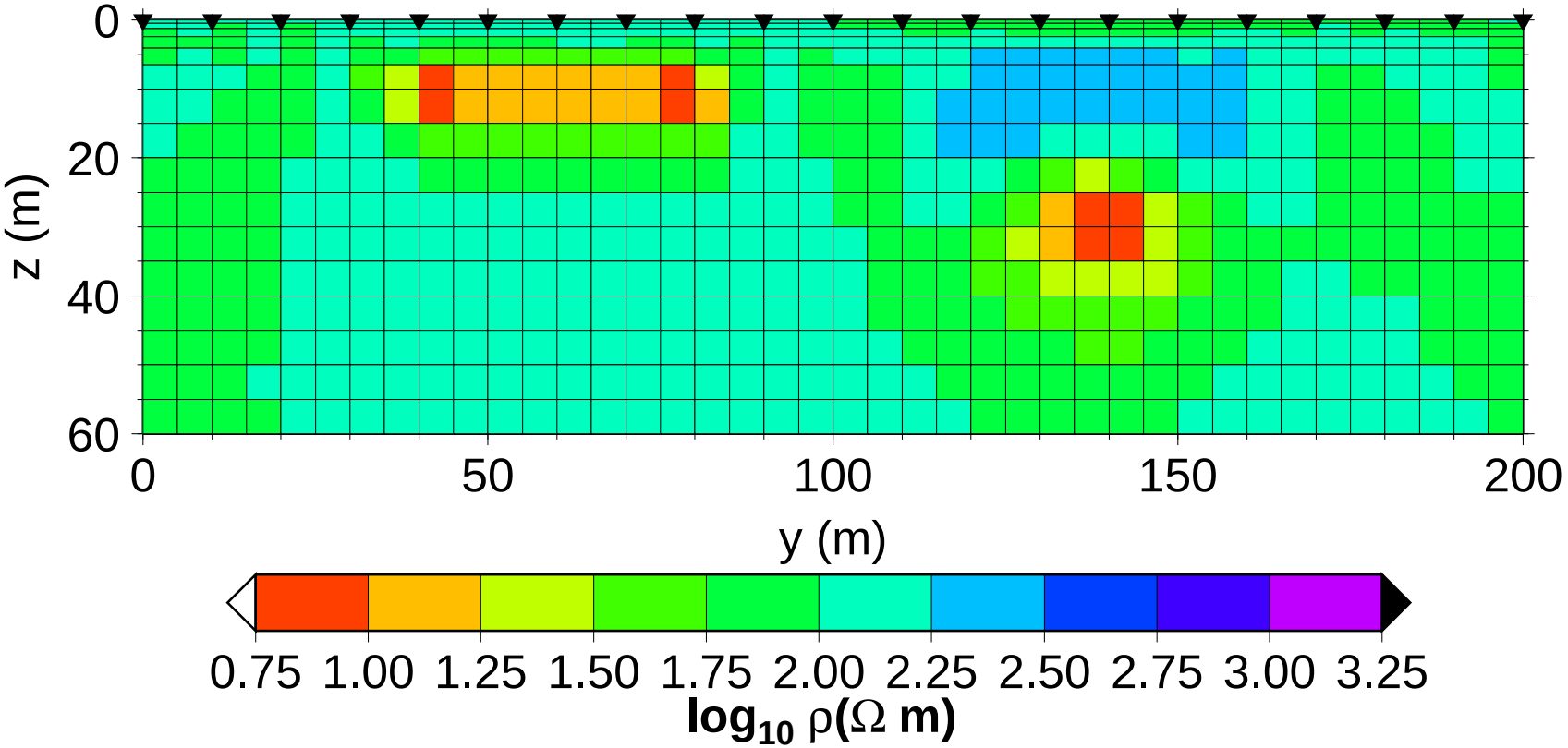

Figure: 2-D Occam inversion result for RMT data; RMS = 1.03.

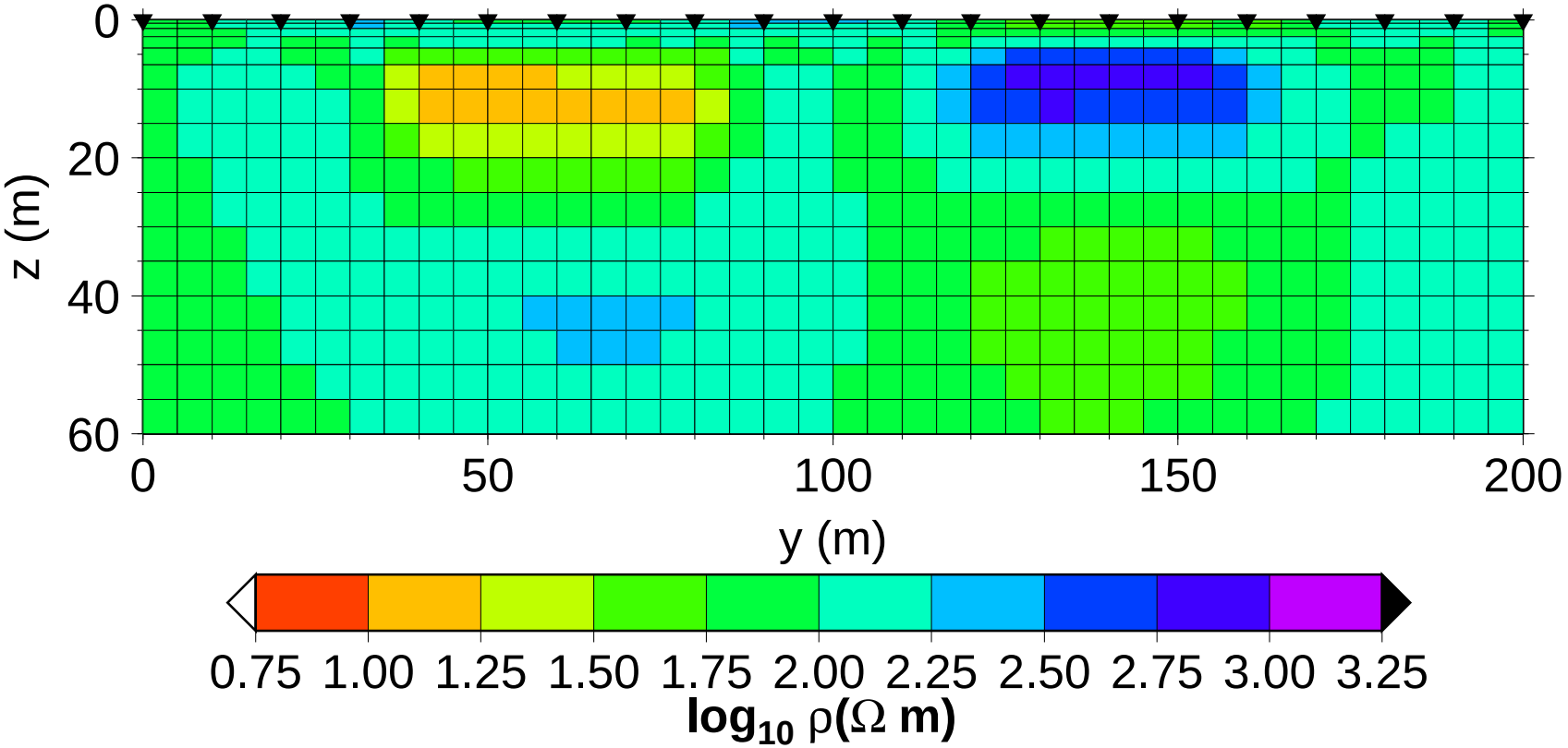

Figure: 2-D Occam inversion result for DCR data; RMS = 1.02.

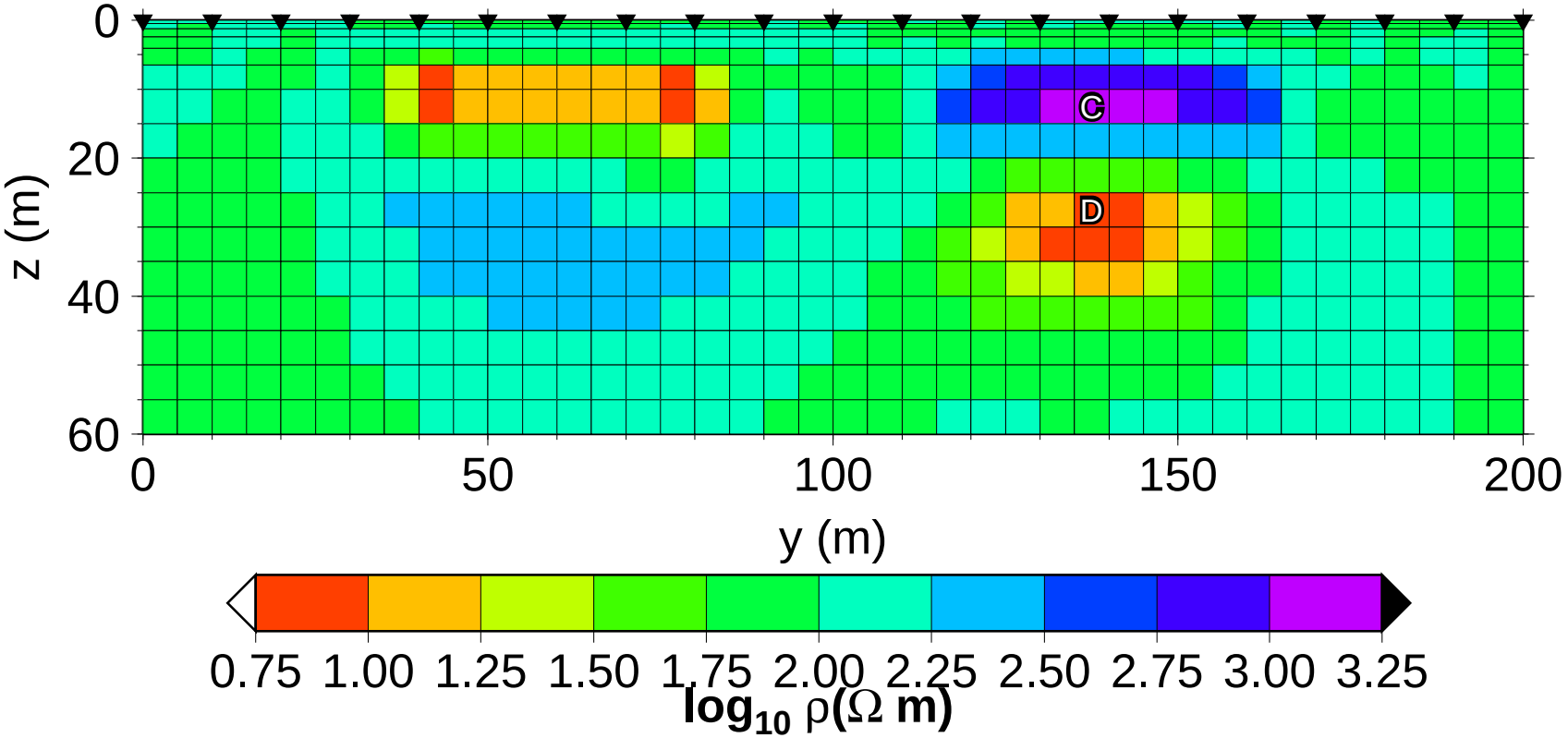

Figure: 2-D Occam joint inversion result for RMT and DCR data; RMS = 0.86.

Non-linear TSVD analysis of parameter C I

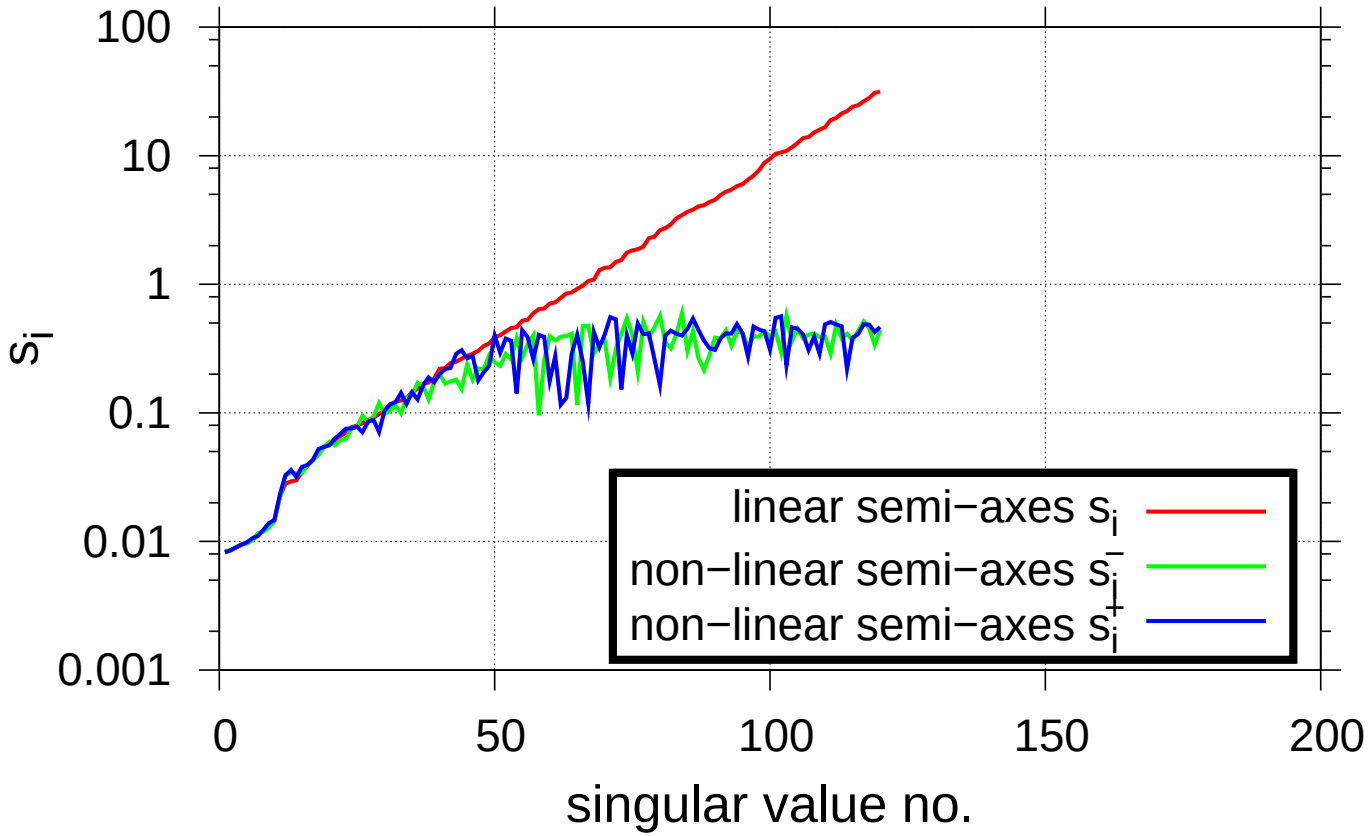

Figure: Linear (red) and non-linear (blue and green) semi-axes from analysis of parameter C in RMT model.

Non-linear TSVD analysis of parameter C II

Results of non-linear error and resolution analyses for parameter C:

	RMT	DCR	joint
p_{cutoff}	120	57	184
f^-_{semi}/f^+_{semi}	1.88/2.00	1.29/1.29	1.97/1.99
f^-_{MSQ}/f^+_{MSQ}	1.89/3.10	1.95/2.44	1.90/4.80

Table: Error factors (f^-_{semi}/f^+_{semi} from non-linear semi-axes, f^-_{MSQ}/f^+_{MSQ} from most-squares inversion) and truncation levels for parameter C ($p_{max} = 234$).

Non-linear TSVD analysis of parameter C III

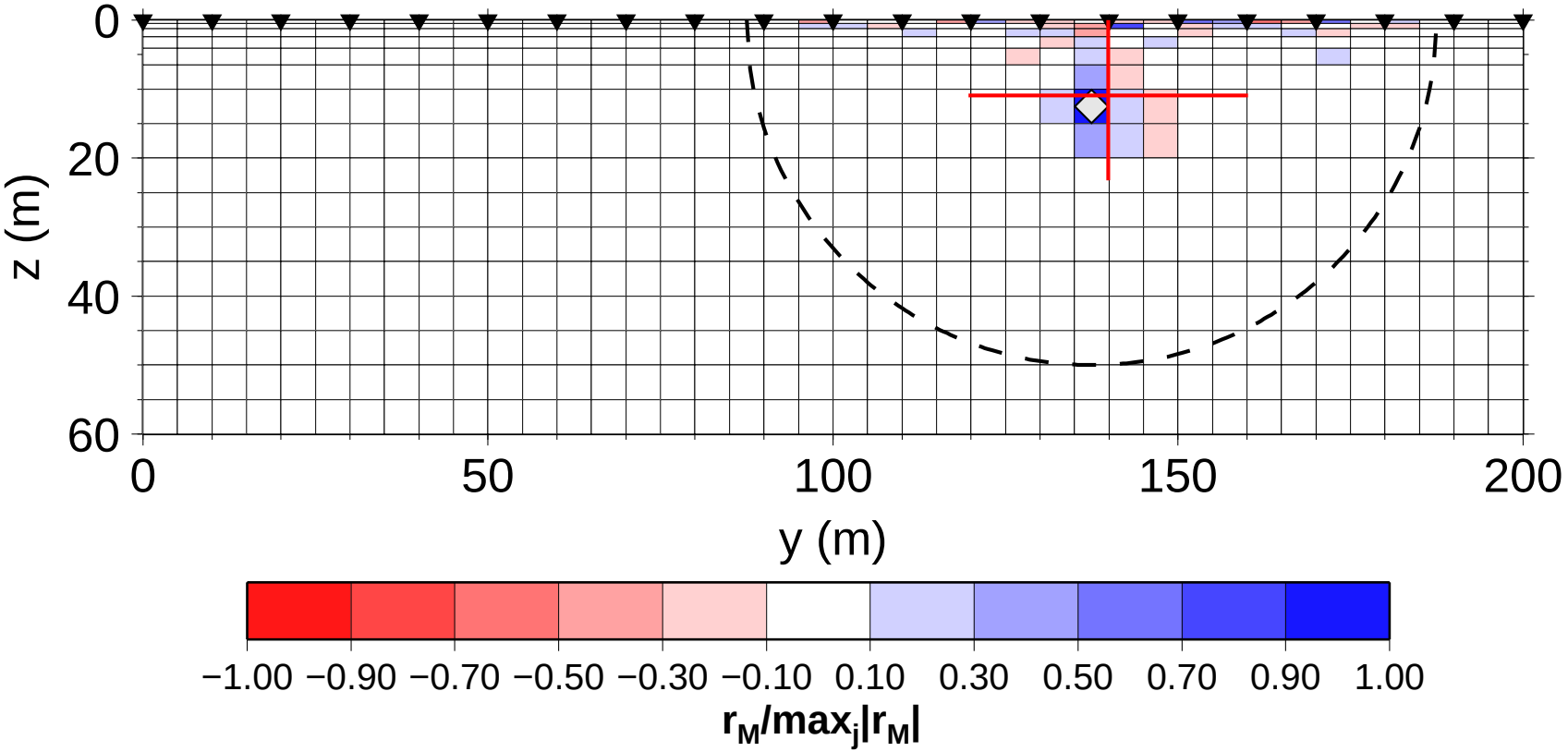

Figure: Resolving kernel of parameter C from RMT inversion.

Non-linear TSVD analysis of parameter C IV

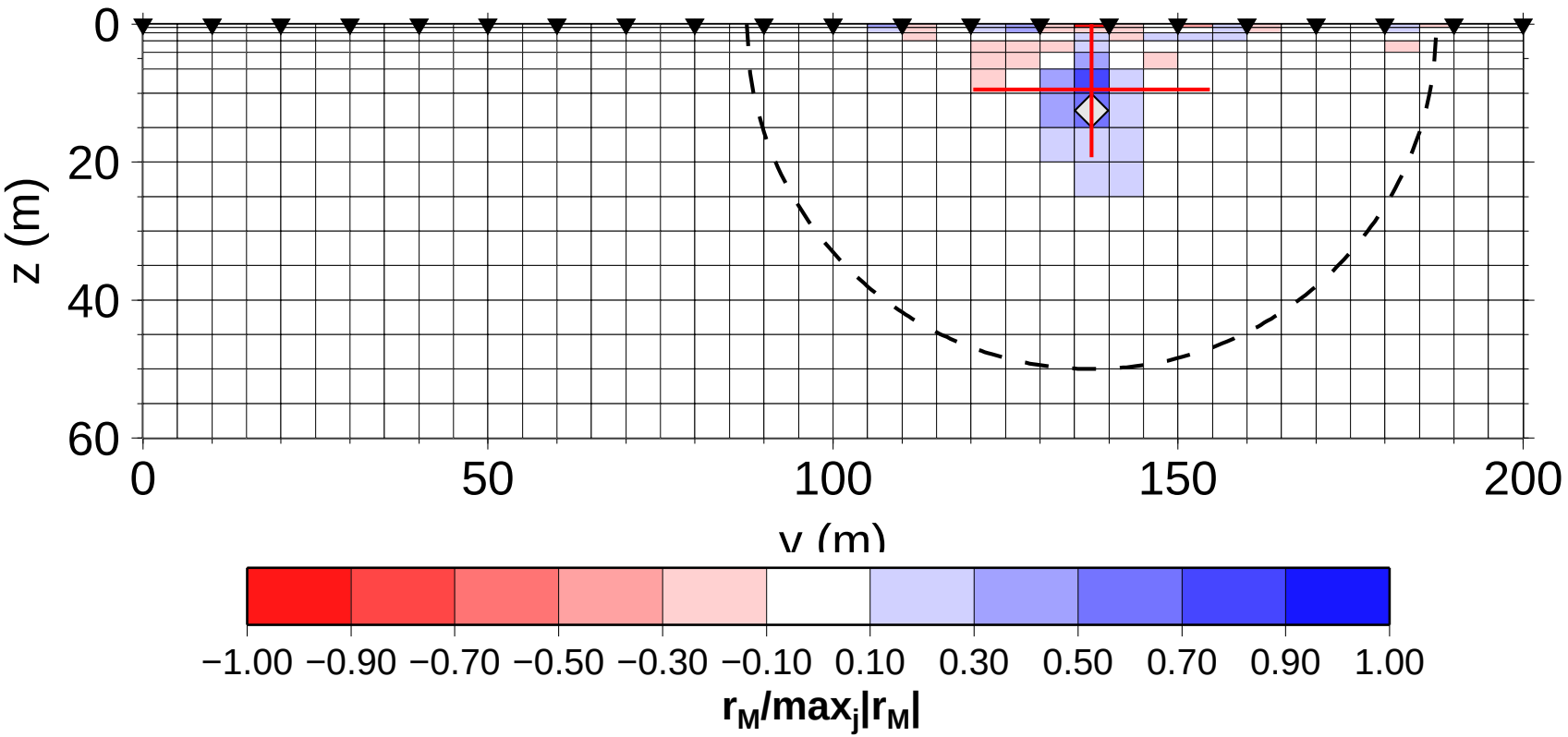

Figure: Resolving kernel of parameter C from DCR inversion.

Non-linear TSVD analysis of parameter C V

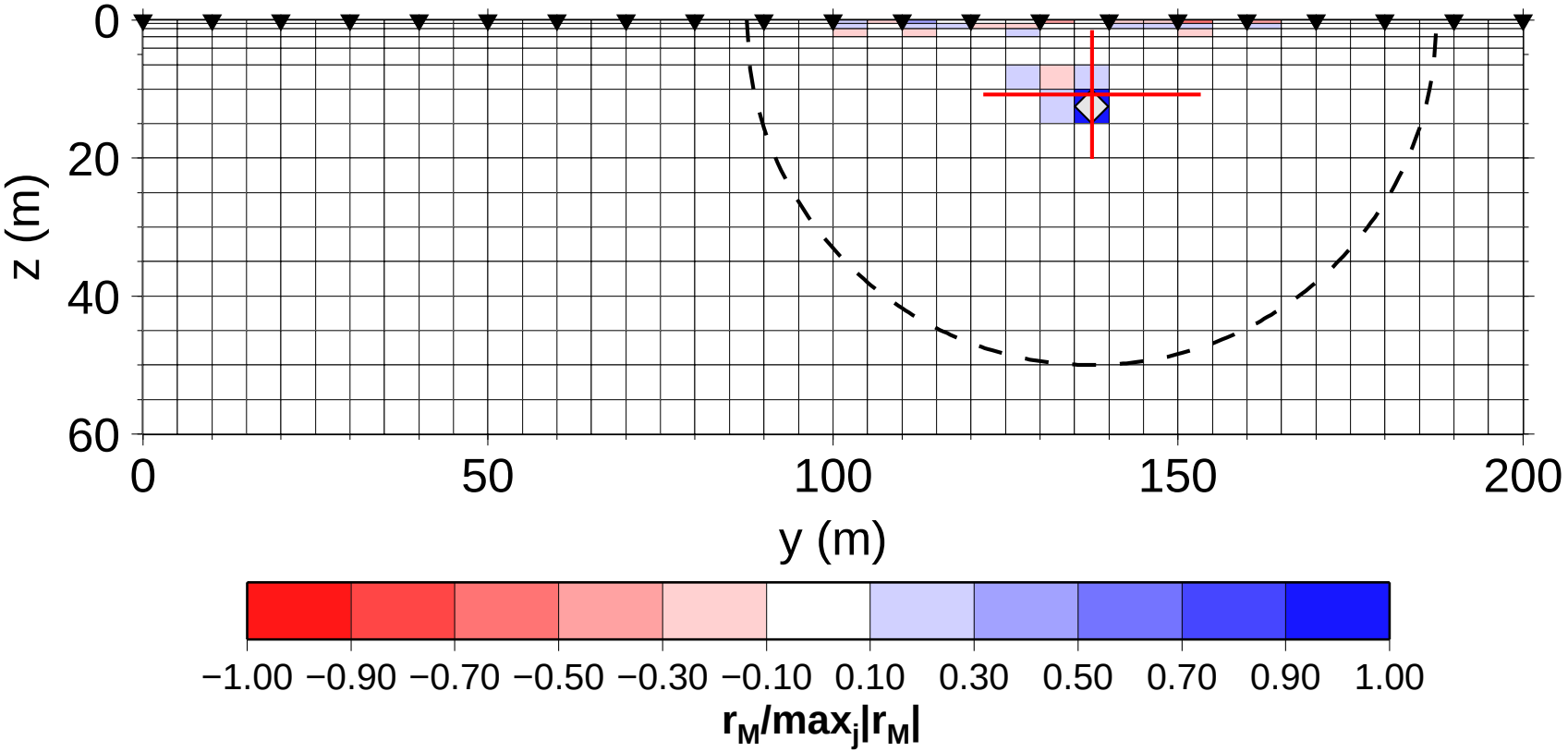

Figure: Resolving kernel of parameter C from joint inversion.

Non-linear TSVD analysis of parameter C VI

	RMT	DCR	joint
p_{cutoff}	120	57	184
$f^{-}_{semi}/f^{+}_{semi}$	1.88/2.00	1.29/1.29	1.97/1.99
f^{-}_{MSQ}/f^{+}_{MSQ}	1.89/3.10	1.95/2.44	1.90/4.80

Table: Error factors ($f^{-}_{semi}/f^{+}_{semi}$ from non-linear semi-axes, f^{-}_{MSQ}/f^{+}_{MSQ} from most-squares inversion) and truncation levels for parameter C ($p_{max} = 234$).

Non-linear TSVD analysis of parameter D I

Results of non-linear variance and resolution analyses for parameter D:

	RMT	DCR	joint
p_{cutoff}	178	72	187
f^-_{semi}/f^+_{semi}	1.9/2.00	1.3/1.3	2.0/2.0
f^-_{MSQ}/f^+_{MSQ}	1.5/1551.5	2.0/2.4	2.0/541.8

Table: Error factors (f^-_{semi}/f^+_{semi} from non-linear semi-axes, f^-_{MSQ}/f^+_{MSQ} from most-squares inversion) and truncation levels for parameter D ($p_{max} = 277$).

Non-linear TSVD analysis of parameter D II

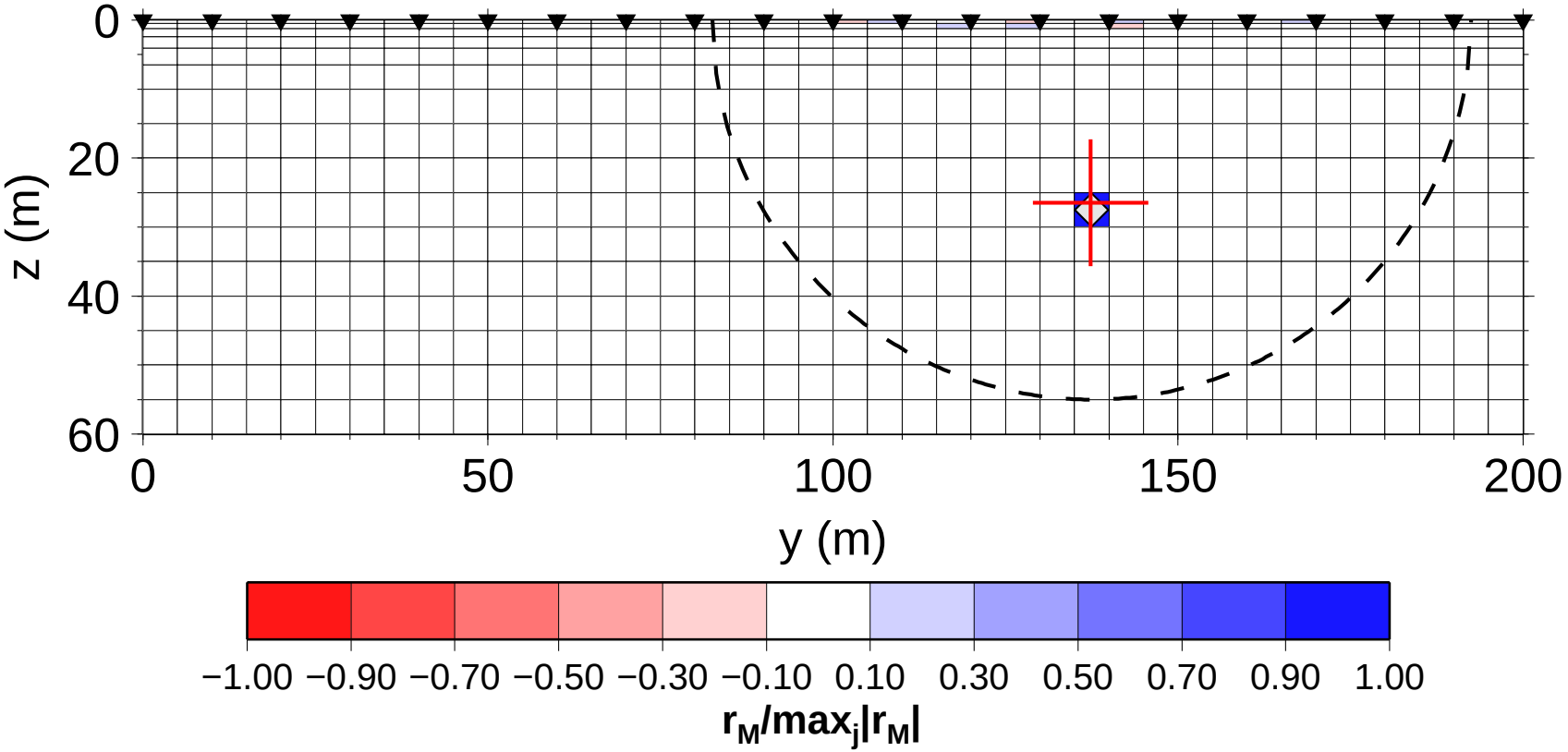

Figure: Resolving kernel of parameter D from RMT inversion.

Non-linear TSVD analysis of parameter D III

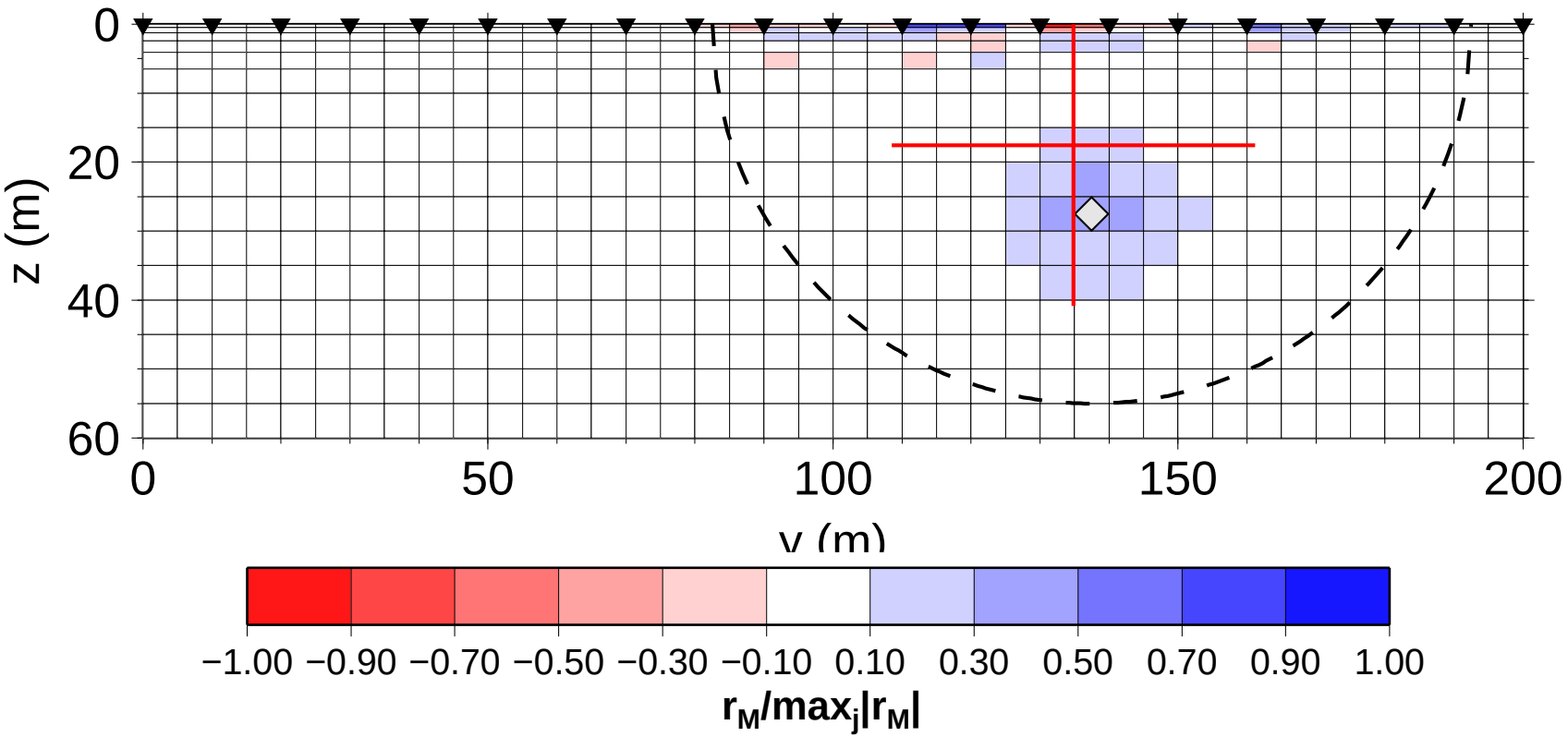

Figure: Resolving kernel of parameter D from DCR inversion.

Non-linear TSVD analysis of parameter D IV

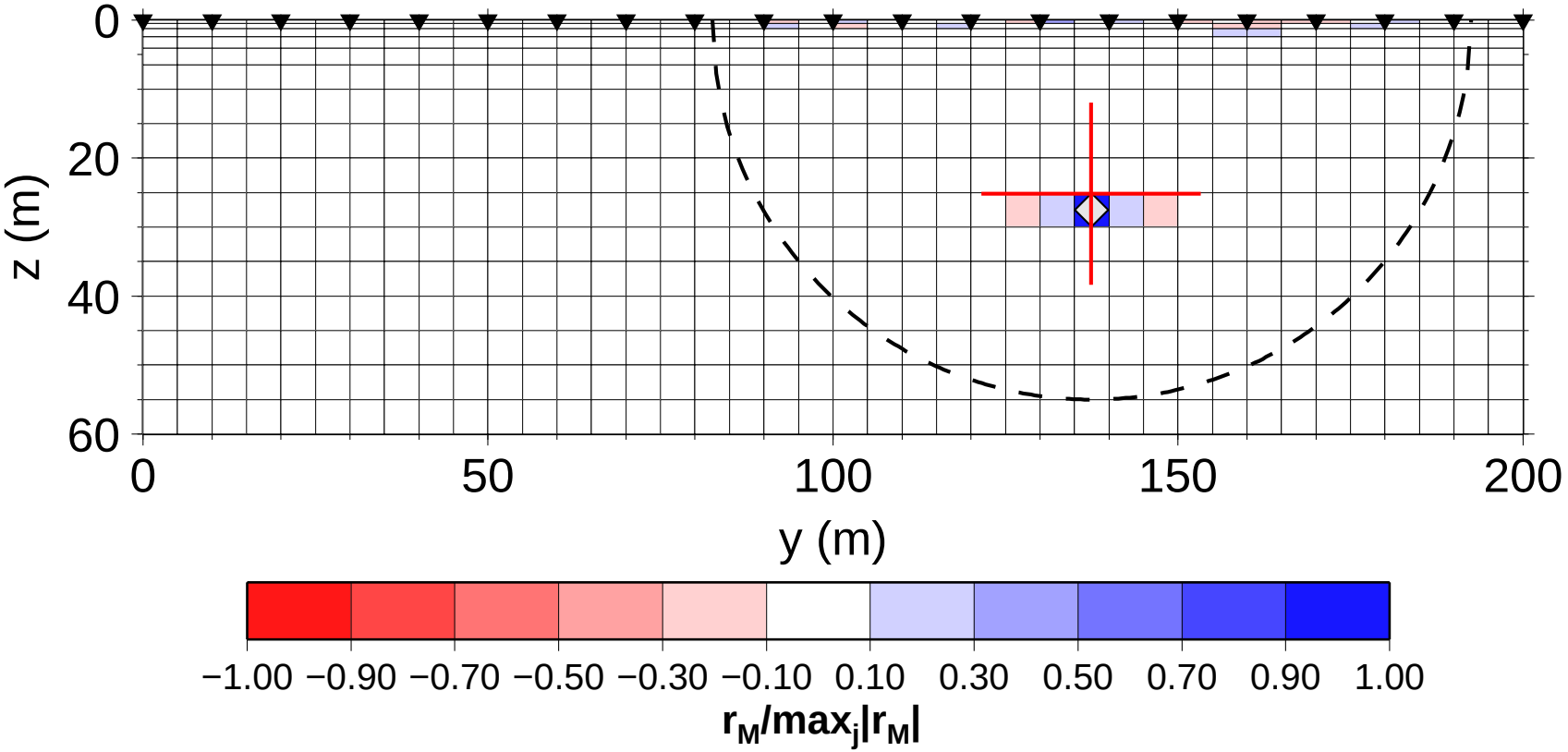

Figure: Resolving kernel of parameter D from joint inversion.

Non-linear TSVD analysis of parameter D V

	RMT	DCR	joint
p_{cutoff}	178	72	187
f^-_{semi}/f^+_{semi}	1.9/2.00	1.3/1.3	2.0/2.0
f^-_{MSQ}/f^+_{MSQ}	1.5/1551.5	2.0/2.4	2.0/541.8

Table: Error factors (f^-_{semi}/f^+_{semi} from non-linear semi-axes, f^-_{MSQ}/f^+_{MSQ} from most-squares inversion) and truncation levels for parameter D ($p_{max} = 277$).

Smoothness-constrained analysis of parameter C I

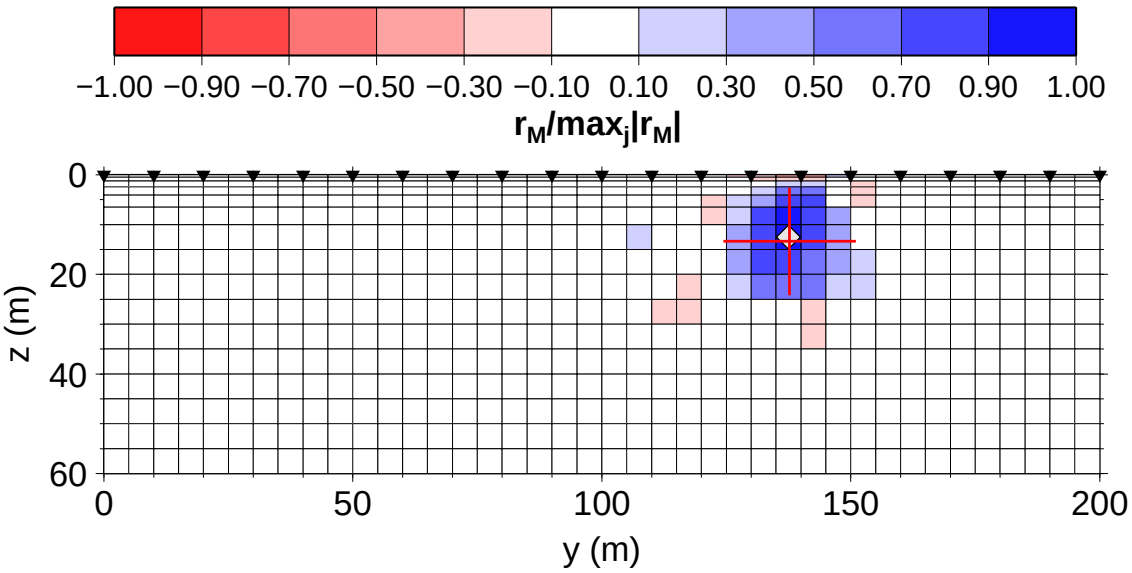

(b) Resolving kernel RMT model

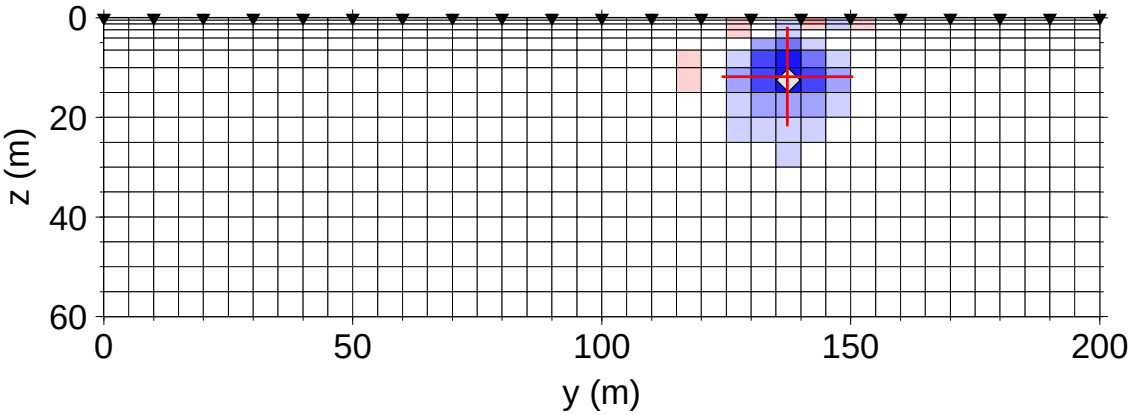

(c) Resolving kernel DCR model

Smoothness-constrained analysis of parameter C II

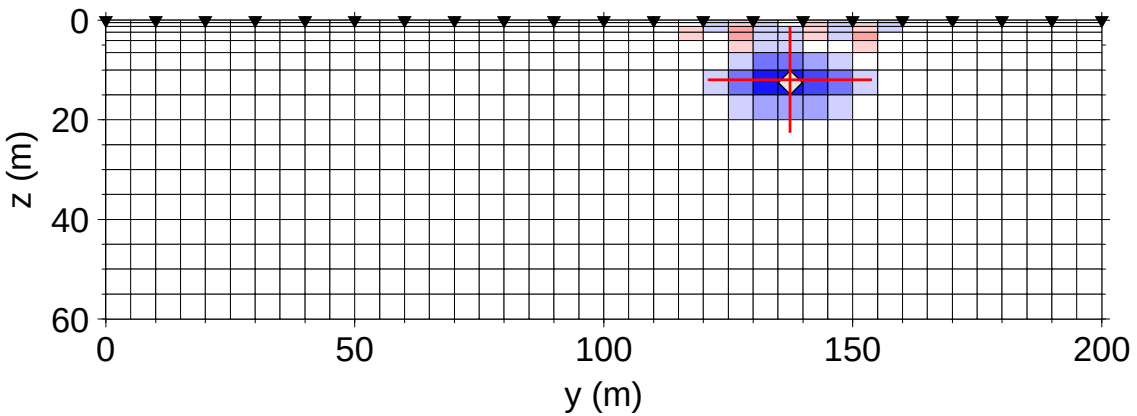

(d) Resolving kernel joint model

	RMT	DCR	joint
f_{lin}	1.26	1.20	1.18
f^{-}_{MSQ}/f^{+}_{MSQ}	1.26/1.26	1.19/1.20	1.15/1.15

(e) Errors

Figure: Resolving kernels and error estimates for parameter C from smoothness-constrained scheme.

Smoothness-constrained analysis of parameter D I

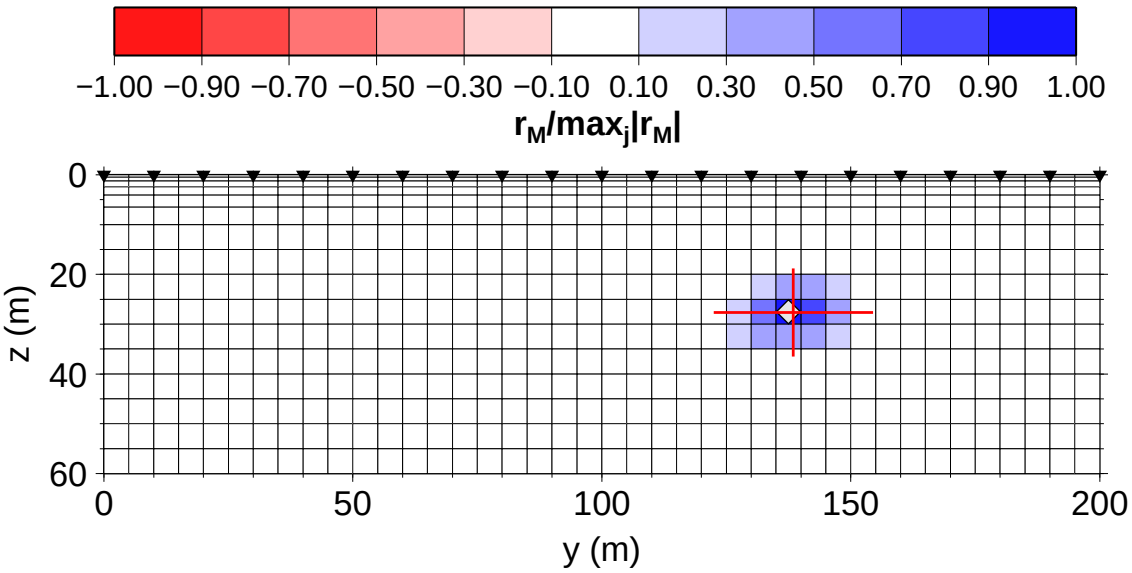

(b) Resolving kernel RMT model

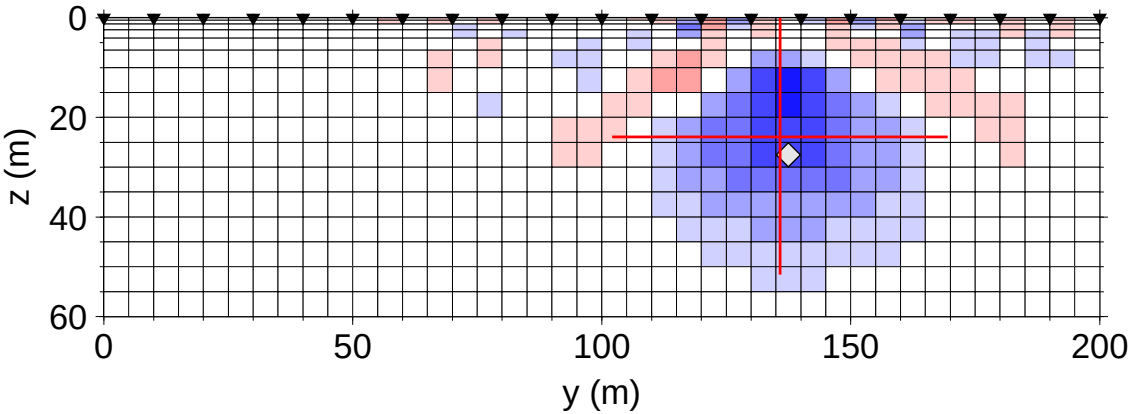

(c) Resolving kernel DCR model

Smoothness-constrained analysis of parameter D II

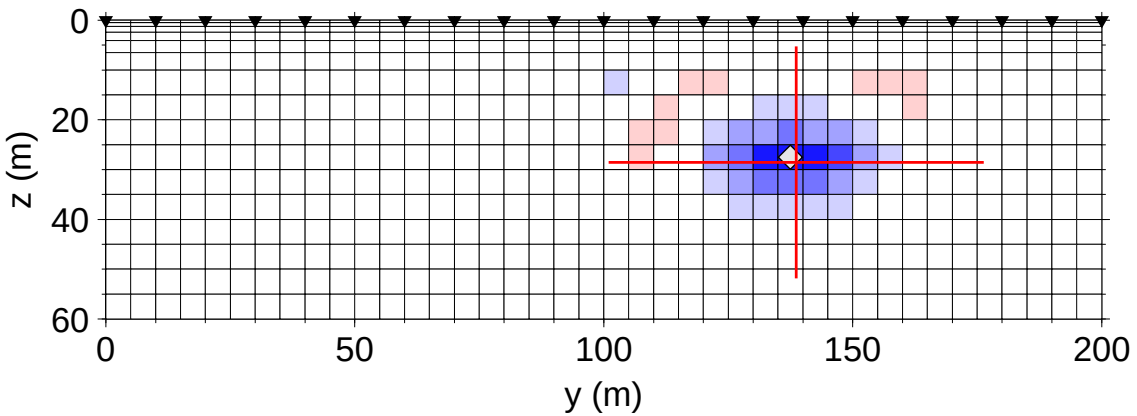

(d) Resolving kernel joint model

	RMT	DCR	joint
f_{lin}	1.18	1.25	1.16
f^{-}_{MSQ}/f^{+}_{MSQ}	1.35/1.39	1.25/1.24	1.27/1.24

(e) Errors

Figure: Resolving kernels and error estimates for parameter D from smoothness-constrained scheme.

Conclusions I

Smoothness-constrained analysis

- Small linearized errors mostly confirmed by most-squares inversion.
- Fairly spread resolving kernels even for shallow structure.

TSVD analysis

- Solely data driven.
- Non-linearity allowed for with semi-axes and most-squares inversion.

Conclusions II

RMT problem

- Non-linearity leads to well constrained models.
- Non-linear errors mostly confirmed by most-squares inversion.

DCR problem

- TSVD based most-squares inversion demonstrates larger model variability than non-linear semi-axes.
- Related to badly determined vertical length scale in DCR models (Parker, 1984)?

Conclusions III

Joint problem

- Improvement of model resolution and error for parameter C in resistive block.
- For parameters outside depth range of investigation of one method, acceptable model error and resolution in joint inversion subject to proper data weighting.

References I

R. L. Parker. The inverse problem of resistivity sounding. *Geophysics*, 49(12):2143–2158, 1984.